Research Article

Cancer Immunology Research

Concurrent PD-1 Blockade Negates the Effects of OX40 Agonist Antibody in Combination Immunotherapy through Inducing T-cell Apoptosis

Rajeev K. Shrimali[1], Shamim Ahmad[1], Vivek Verma[1], Peng Zeng[1], Sudha Ananth[1], Pankaj Gaur[1], Rachel M. Gittelman[2], Erik Yusko[2], Catherine Sanders[2], Harlan Robins[2,3], Scott A. Hammond[4], John E. Janik[1], Mikayel Mkrtichyan[1], Seema Gupta[1], and Samir N. Khleif[1]

Abstract

Combination therapies that depend on checkpoint inhibitor antibodies (Abs) such as for PD-1 or its ligand (PD-L1) together with immune stimulatory agonist Abs like anti-OX40 are being tested in the clinic to achieve improved antitumor effects. Here, we studied the potential therapeutic and immune effects of one such combination: Ab to PD-1 with agonist Ab to OX40/vaccine. We tested the antitumor effects of different treatment sequencing of this combination. We report that simultaneous addition of anti–PD-1 to anti-OX40 negated the antitumor effects of OX40 Ab. Antigen-specific $CD8^+$ T-cell infiltration into the tumor was diminished, the resultant antitumor response weakened, and survival reduced. Although we observed an increase in IFNγ-producing E7-specifc $CD8^+$ T cells in the spleens of mice treated with the combination of PD-1 blockade with anti-OX40/vaccine, these cells underwent apoptosis both in the periphery and the tumor. These results indicate that anti–PD-1 added at the initiation of therapy exhibits a detrimental effect on the positive outcome of anti-OX40 agonist Ab. These findings have important implications on the design of combination immunotherapy for cancer, demonstrating the need to test treatment combination and sequencing before moving to the clinic. *Cancer Immunol Res; 5(9); 755–66. ©2017 AACR.*

Downloaded from http://aacrjournals.org/cancerimmunolres/article-pdf/5/9/755/2352265/755.pdf by guest on 26 August 2022

Introduction

Immunotherapy has emerged as an effective treatment modality for cancer and has improved long-term survival in some patients. Effective antitumor immunity depends mainly on effector T cells whose fate is mediated by the interaction of immune inhibitory and stimulatory receptors or their ligands (1, 2). Antibodies (Abs) against programmed cell death protein 1 (PD-1) or one of its ligands (i.e., PD-L1) have generated clinical responses and an increase in survival in many types of cancers (3–5). However, anti–PD-1/PD-L1 Ab as a single agent is not sufficient to improve clinical outcome in most patients, emphasizing the need to develop combination immunotherapy strategies (4, 5). Combination therapies with two checkpoint inhibitor Abs, anti–PD-1 and anti-cytotoxic T lymphocyte–associated protein 4 (CTLA-4), resulted in an increase in the response rate but severe immune-associated adverse events were also reported (3, 6).

T-cell costimulation through receptors, such as OX40, GITR, or 4-1BB, provides a potent stimulatory signal that promotes the expansion and proliferation of killer $CD8^+$ and helper $CD4^+$ T cells (7). OX40 is a tumor necrosis factor receptor superfamily member 4 (TNFRSF4) that promotes activation and expansion of T cells leading to enhanced effector functions, memory generation, and immune inflammatory antitumor responses (8–11). Agonist antibody to OX40 alone or in combination with other immune-modulatory Abs is being tested against various types of cancers in early phase clinical trials (8). The combination of checkpoint inhibitor Abs, anti–PD-1 or anti–PD-L1, and anti-OX40 agonist Ab are candidates for combination immunotherapy. Few clinical trials have started and others are being planned to test this combination. However, response results have not yet been reported (12, 13). Further, the potential immune effect of such combination and the interaction of the two molecules on the downstream immune outcome are not fully clear. Furthermore, several challenges remain to determine whether the positive outcome of any of the immune modulator single agents is positively or negatively affected when combined with another immune modulating agent. Therefore, there is a need to identify

[1]Georgia Cancer Center, Augusta University, Augusta, Georgia. [2]Adaptive Biotechnologies, Seattle, Washington. [3]Computational Biology Program, Fred Hutchinson Cancer Research Center, Seattle, Washington. [4]MedImmune LLC, Gaithersburg, Maryland.

Note: Supplementary data for this article are available at Cancer Immunology Research Online (http://cancerimmunolres.aacrjournals.org/).

R.K. Shrimali and S. Ahmad contributed equally to this article.

Current address for R.K. Shrimali: Peloton Therapeutics, Dallas, Texas; and current address for M. Mkrtichyan: Five Prime Therapeutics Inc., South San Francisco, California.

Corresponding Author: Samir N. Khleif, Augusta University, 1410 Laney Walker Boulevard, Augusta GA 30912. Phone: 706-721-0570; Fax: 706-721-8787; E-mail: SKhleif@augusta.edu

doi: 10.1158/2326-6066.CIR-17-0292

©2017 American Association for Cancer Research.

ideal partners for combination immunotherapy, and standardize their dosage and sequencing to achieve maximum treatment efficacy.

Here, we tested the effect of adding anti–PD-1 on agonist anti-OX40 activity with a vaccine when combined for therapeutic intent in the TC-1 tumor model. We found that the concurrent administration of anti–PD-1 with anti-OX40 agonist Ab and vaccine inhibits the positive effect of anti-OX40 on the immune response and suppresses its antitumor therapeutic efficacy. We further found that simultaneous blocking of PD-1/PD-L1 pathway with OX40 activation drives T cells into apoptosis *in vitro* and *in vivo*, which leads to abolishing of the therapeutic effect of agonist OX40 Ab/vaccine. Furthermore, we report that a delayed treatment schedule of anti–PD-1 did not improve the antitumor effects of the anti-OX40 and vaccine regimen.

Materials and Methods

Mice

C57BL/6 female mice 6 to 8 weeks old were purchased from The Jackson Laboratory and housed under pathogen-free conditions. *In vitro* experiments used pMel-1 mice [B6.Cg-Thy1^a/Cy Tg (TcraTcrb)8Rest/J] that carry a rearranged TCR transgene (*Vβ13*) specific for the mouse homolog (*pmel-17*) of human *gp100* (14). All procedures were carried out in accordance with approved Augusta University IACUC animal protocols.

Tumor cell line

TC-1 cells that were derived by stable transfection of mouse lung epithelial cells with human papillomavirus strain 16 (HPV16) early proteins 6 and 7 (E6 and E7) and activated h-ras oncogene were obtained from Dr. T-C Wu (Johns Hopkins University; ref. 15). Cells were grown in RPMI 1640 supplemented with 10% FBS, 2 mmol/L L-glutamine, penicillin (100 U/mL) and streptomycin (100 μg/mL) at 37°C with 5% CO_2 and maintained at a confluence of 70% to 80%. These cells were tested routinely for absence of mycoplasma by using PCR at Georgia Cancer Center, Augusta University (Augusta, GA). All tests were negative.

Vaccines

The CTL epitope from HPV16 $E7_{49–57}$ (9 amino acid (aa) peptide, RAHYNIVTF, 100 μg/mouse) mixed with synthetic T helper epitope PADRE (13 aa peptide, aK-Cha-VAAWTLKAAa, where "a" is D alanine and Cha is L-cyclohexylalanine, 20 μg/mouse; both from Celtek Bioscience) and QuilA adjuvant (20 μg/mouse; Brenntag) were used as the model vaccine in all experiments (16). Three doses of vaccine were administered subcutaneously (s.c.), every seven days (D) in tumor-bearing mice. The $gp100_{25–33}$ 9-mer peptide (KVPRNQDWL; ANASPEC Inc.) was used for *in vitro* activation of magnetically enriched $CD8^+$ T cells from spleens of pMel-1 mice (14). The purity of the enriched cells was more than 90%.

Abs and reagents

Purified anti-mouse anti–PD-1 (RMP1-14 clone, Rat IgG2a) was obtained from Biolegend. Anti-OX40 (clone OX86, Rat IgG1) was obtained from MedImmune. Live/Dead Fixable cell stain kit was obtained from Invitrogen, ThermoFisher Inc. Appropriately fluorochrome-labeled anti-mouse Abs against CD45, CD3, CD4, CD8, Annexin, Foxp3, PD-1, PD-L1, and OX40 were obtained from BD Biosciences for flow cytometric measurements. Intracellular Foxp3 staining kit was obtained from eBiosciences and E7 FITC dextramers were from Immudex. $CD8^+$ enrichment kits (Miltenyi) were used per manufacturer's instructions.

Tumor implantation, immunization, Ab treatment, and tumor volume measurement

In the therapeutic experiments, mice were implanted with 70,000 TC-1 cells/mouse s.c. into the right flank at D0. Ten to twelve days (D10–D12) later, when tumors measured approximately 6 to 8 mm in diameter, mice from appropriate groups (5 mice per group) were injected with vaccine (s.c., total 3 doses, 1 week apart). Anti–PD-1 was administered intraperitoneally (i.p.) twice weekly throughout the experiment at a dose of 1 mg/kg beginning either at the time of first or second (Late; L) vaccination. Agonist anti-OX40 was administered i.p. twice weekly throughout the experiment at a dose of 1 mg/kg beginning with the first vaccination (continuous; C). In some experiments, anti-OX40 administration was stopped after the second vaccination (Short-term; ST). Tumors were measured every 3 to 4 days using a digital vernier caliper and the tumor volume was calculated using the formula: $V = L \times W^2/2$, where V is tumor volume, L is the length of tumor (longer diameter) and W is the width of the tumor (shorter diameter). Mice were monitored for tumor growth and survival. Mice were sacrificed when tumors reached 1.5 cm^3 in volume or tumors became ulcerated or when mice became moribund.

For immune response experiments, mice were treated following the same schedule as for the therapy experiment, except only two doses of weekly vaccines were given to be able to collect tissues from control animals before their tumors reach a volume of 1.5 cm^3. Three days after the second vaccination, mice from the appropriate groups were euthanized to harvest spleens and tumors, which were further processed using GentleMACS dissociator and the solid tumor homogenization protocol, as suggested by the manufacturer (Miltenyi Biotec). Each experiment was repeated at least twice.

Flow cytometric analysis of tumor-infiltrating lymphocytes

One million cells were stained for live and dead staining (Invitrogen, ThermoFisher Inc.) followed by Foxp3 fixation and permeabilization, which were done according to the manufacturer's (BD Pharmingen) protocol. Intracellular staining for Foxp3 was performed using anti–Foxp3-APC monoclonal Ab (eBioscience). Data acquisition was performed on FACSCalibur or LSRII (BD Biosciences). Results were analyzed with CellQuest (BD Biosciences) or FlowJo (TreeStar). Total number of $CD3^+$, $CD8^+$, $CD4^+$, $CD8^+E7^+$, and $CD4^+Foxp3^+$ cells were analyzed within a $CD45^+$ hematopoietic cell population and represented in 1×10^6 live cells in tumors.

Enzyme-linked immunosorbent (ELISpot) assay

IFNγ production in E7 restimulated (10 μg/mL) splenocyte cultures from various treatment groups was detected by ELISpot assay performed as suggested by the manufacturer (BD Biosciences). In brief, splenocytes from variously treated groups were incubated with ACK lysis buffer for 5 minutes to lyse red blood cells. Following lysis, cells were washed, filtered, counted, and 0.4×10^6 cells were plated along with E7 peptide in anti-IFNγ coated plates at 37°C/5% CO_2 for 24 hours. Plates were washed, blocked, and further developed with anti-IFNγ detection Ab using

Downloaded from http://aacrjournals.org/cancerimmunolres/article-pdf/5/9/755/2352265/755.pdf by guest on 26 August 2022

biotin-streptavidin-HRP complex. Finally, plates were washed and allowed to dry for spots to develop. Spots were counted and analyzed using CTL Immunospot Analyzer (Cellular Technology), and results were examined for differences of E7-specific IFNγ spots between various treatment groups. One set of samples were also activated with DMSO as a control.

Analysis of proliferation and apoptosis

For *in vitro* activation, magnetically enriched (Miltenyi Biotec) $CD8^+$ T cells (>95% purity) from pMel-1 mice were stimulated *in vitro* by $gp100_{25–33}$ peptide at 0.01 μmol/L concentration (day 0) for 48 hours. For this $CD8^+$ T cells were cultured in T-cell medium containing RPMI-1640 (Lonza) supplemented with 10% fetal bovine serum (FBS), penicillin (100 U/mL), streptomycin (100 mg/mL), 0.1% β-mercaptoethanol (Life Technologies, Invitrogen), and IL2 (100 U/mL; Peprotech) at 37°C/5% CO_2. This activation step was followed by a resting period of 24 hours during which activated cells were cultured in IL2-containing T-cell medium. At various time points, samples were collected for analyzing the expression of PD-1, PD-L1, and OX40 using FACS. Following the resting period, cells were further cultured with 0.2 μmol/L $gp100_{25-33}$ for 96 hours, with or without anti–PD-1 and/or anti-OX40. In some assays, after resting period, cells were rechallenged with $gp100_{25-33}$ peptide for 24 hours in combination with anti–PD-1 and/or anti-OX40 followed by further incubation with these Abs for 48 hours. In all experimental setups, at the end of incubation, cells were harvested for either FACS or Western blot analyses. For determination of apoptosis, activated cells were stained for cell surface markers including fixable live/dead staining and washed once in 1X PBS, then once in 1X Annexin V Binding Buffer (eBioscinces). Cells were incubated for 10 to 15 minutes in 100 μL of Annexin V binding buffer containing 3 μL of APC-conjugated Annexin V at room temperature and protected from light. Moreover, in some assays, cell proliferation was determined by using CellTtrace Violet (CTV) cell proliferation kit (Invitrogen, ThermoFisher Inc.) using FACS analysis. Results for cell proliferation were normalized for three independent experiments. For negative control, non-stimulated (NS) cells were left in media containing IL2 for duration of the experiment.

For determination of apoptosis *in vivo*, $CD8^+$ T cells from tumors and spleens of variously treated mice were processed into single-cell suspensions as explained above followed by Annexin V–positive-APC staining in Annexin V binding buffer and FACS acquisition as described above.

Western blot analysis

After final restimulation, $CD8^+$ T cells in the various groups were harvested and treated with cell lysis buffer (RIPA buffer + 1% phosphatase inhibitor + 1% protease inhibitor) for preparing the cell lysates. Protein concentrations in the various cell lysates were determined by Pierce BCA Protein Assay Kit (ThermoFisher Scientific). Twenty to thirty microgram protein was loaded onto Novex 4% to 20% Tris-Glycin Mini Gels (ThermoFisher Scientific) followed by transfer onto nitrocellulose membranes. Membranes were blocked with 3% BSA in Tris-buffer followed by overnight probing of the proteins with Abs directed against mouse-pro–caspase 3, cleaved caspase 3, Bcl-xL, and β-actin. All Abs were purchased from Cell Signaling Technology. Blots were developed with rabbit anti-mouse horseradish peroxidase (HRP) labeled secondary Abs.

T-cell receptor variable β chain sequencing

Three days after second vaccination tumors and spleens were harvested and single-cell suspensions were prepared as described above for immune response studies. Cells were then sent to Adaptive Biotechnologies as frozen samples in freezing medium (10% DMSO in FBS) for T-cell receptor (TCR) variable β-chain sequencing. Immunosequencing of the CDR3 regions of mouse TCRβ chains was performed using the ImmunoSEQ Assay (Adaptive Biotechnologies). Extracted genomic DNA was amplified in a bias-controlled multiplex PCR, followed by high-throughput sequencing. Sequences were collapsed and filtered in order to identify and quantitate the absolute abundance of each unique TCRβ CDR3 region for further analysis as previously described (17–19).

Statistical analysis

All statistical parameters (average values, SD, SEM, significant differences between groups) were calculated using GraphPad Prism or Excel as appropriate. Statistical significance between groups was determined by Student *t* test or one-way ANOVA with Tukey's multiple comparison post-test ($P \leq 0.05$ was considered statistically significant). Survival in various groups was compared using GraphPad Prism using log-rank (Mantel–Cox) test. SK plots were generated by internally developed software (https://skylineplotter.shinyapps.io/SkyLinePlotter/). Contrary to the survival plot made using GraphPad Prism, the SK plot gives dynamic simultaneous presentation of tumor volumes and mouse survival at a specific time point.

For statistical analyses of TCR-β sequencing results, clonality was defined as 1- Peilou's evenness and was calculated on productive rearrangements by $1 + \frac{\sum_i^N p_i \log_2(p_i)}{\log_2(N)}$ where p_i is the proportional abundance of rearrangement *i* and *N* is the total number of rearrangements (20). Clonality values range from 0 to 1 and describe the shape of the frequency distribution: clonality values approaching 0 indicate a very even distribution of frequencies, whereas values approaching 1 indicate an increasingly asymmetric distribution in which a few clones are present at high frequencies. To estimate the fraction of T cells in the tissue samples, we considered 6.5 pg of DNA per diploid cell, which is equal to approximately 154 productive TCR loci per ng of DNA, and normalized the total T-cell estimates in each sample to the amount of input DNA multiplied with the value of 154 productive TCR loci per ng of input DNA.

Results

Antitumor effects of anti-OX40/vaccine are negated by anti–PD-1

To evaluate the antitumor therapeutic response of the anti-OX40 agonist Ab, we used the TC-1 syngeneic mouse model. Because the TC-1 model requires vaccine to generate an effector immune response, we first combined the anti-OX40 with an HPV16 E7 peptide vaccine (Fig. 1A). Both the anti-OX40 and the vaccine were administered simultaneously on D12 (Fig. 1A). Although neither E7 vaccine nor anti-OX40 alone affected tumor growth, OX40 Ab in combination with vaccine led to significant ($P \leq 0.05$) slowdown of tumor progression (Fig. 1B and C) associated with prolonged survival (Fig. 1D and E). Although none of the mice survived for more than 30 days following vaccine or anti-OX40 treatments, about 80% of the mice were alive at

Downloaded from http://aacrjournals.org/cancerimmunolres/article-pdf/5/9/755/2352265/755.pdf by guest on 26 August 2022

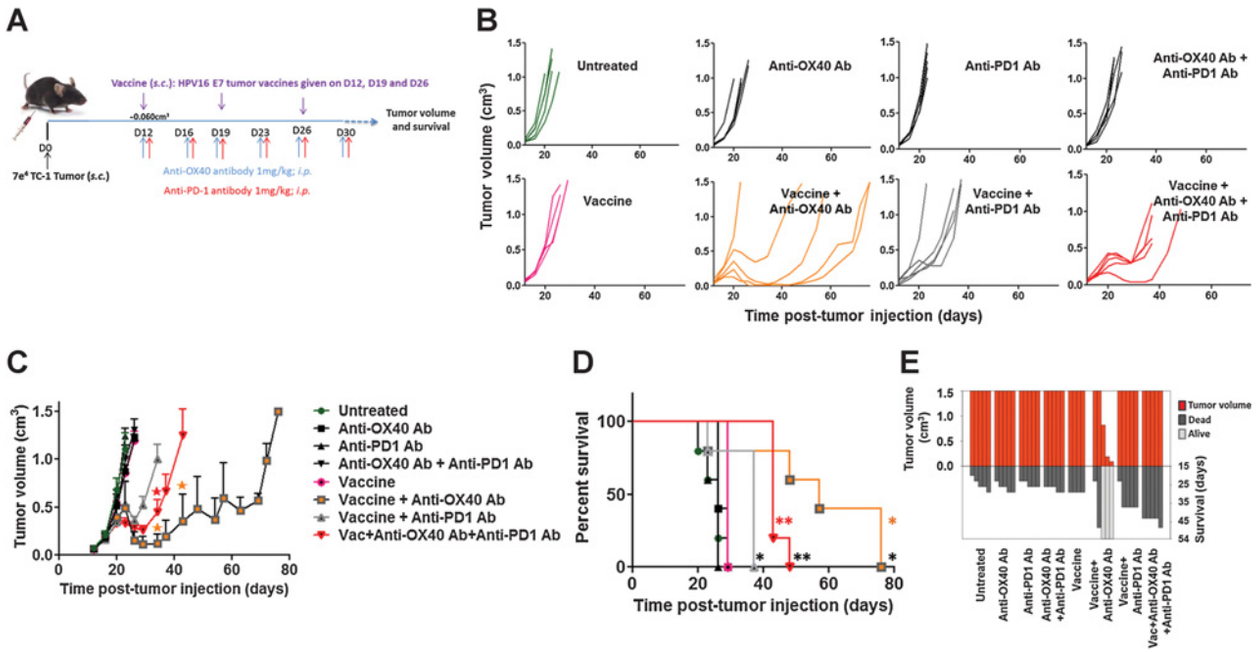

Figure 1.

Effects of agonist OX40 Ab/vaccine and anti–PD-1 on tumor growth and survival. **A,** Schematic representation of the treatment schedule in TC-1 tumor model. On day 12 of tumor growth, TC-1 tumor bearing mice were given anti-OX40 or anti–PD-1 (1 mg/kg, i.p., twice weekly) with HPV17 $E7_{49\text{-}57}$ peptide vaccine administered along with PADRE and QuilA s.c., every 7 days for a total of 3 doses. Tumor growth and survival were measured. **B,** Tumor volume in individual mice and **C,** averaged tumor volumes following various treatments ($n = 5$ per group). **D,** Percent survival of mice depicted by the Kaplan–Meier plot. **E,** SK Plot showing the tumor volume and survival for each mouse at different days. Similar results were obtained from two independent experiments. *, $P \leq 0.05$; **, $P \leq 0.01$; ***, $P \leq 0.001$; ****, $P \leq 0.0001$; *vs. untreated (UT), *vs. vaccine + anti–PD-1, *vs. vaccine + anti-OX40+anti–PD-1; i.p., intraperitoneal; s.c., subcutaneous.

day 40 following anti-OX40/vaccine treatment (Fig. 1D and E). With the intention to further enhance the antitumor effects of OX40 Ab, tumor-bearing mice were concomitantly treated with anti–PD-1 together with anti-OX40/vaccine on day 12 (Fig. 1A). Surprisingly, the antitumor effects observed after simultaneous treatment of tumor-bearing mice using anti–PD-1 and anti-OX40/vaccine were significantly less than the effects observed after anti-OX40/vaccine treatment ($P \leq 0.05$; Fig. 1B and C). Although 60% of the mice survived following anti-OX40/vaccine treatment, addition of anti–PD-1 led to a reduction of survival to only 20% at day 50 (Fig. 1D and E). Accordingly, the addition of anti–PD-1 negated the effect of anti-OX40/vaccine on both tumor-growth inhibition and survival when administered simultaneously.

Anti-OX40/vaccine–induced T-cell infiltration into tumors is reduced by checkpoint blockade

To understand the mechanisms underlying the negative effects of PD-1 blockade on anti-OX40 treatment, we compared the infiltration of immune cells in the tumor microenvironment (TME) following combination treatment. In accordance with the therapeutic response obtained following agonist anti-OX40 treatment in combination with E7 vaccine, a significant increase in number of tumor-infiltrating $CD3^+$ T cells was observed compared with monotherapies (vaccine; $P \leq 0.001$ or anti-OX40; $P \leq 0.0001$; Fig. 2A). Similar results were obtained for $CD4^+$ and $CD4^+Foxp3^-$ T cells with maximum increase following anti-OX40 in combination with the vaccine (Fig. 2B and C). However, the numbers of tumor-infiltrating $CD3^+$, $CD4^+$, and $CD4^+Foxp3^-$ T cells were significantly reduced following the addition of PD-1 blockade to anti-OX40/vaccine combination ($P \leq 0.05$ for each subset of T cells; Fig. 2A–C). This result further reflects the negative therapeutic effect obtained following the addition of anti–PD-1 to anti-OX40. We also found that PD-1 blockade significantly reduced the number of tumor-infiltrating $CD8^+$ ($P \leq 0.01$) and antigen-specific $E7^+CD8^+$ T cells ($P \leq 0.05$) induced by anti-OX40/vaccine treatment (Fig. 2D and E). Finally, adding anti–PD-1 to anti-OX40/vaccine did not affect the tumor infiltration of $Foxp3^+CD4^+$ T regulatory cells (Tregs; Fig. 2F), although the ratio of $CD8^+$/Treg, a well-established criteria that correlates with cancer prognosis (21–24), was significantly reduced due to the decrease in $CD8^+$ T cells tumor infiltration ($P \leq 0.05$; Fig. 2G). Moreover, the $E7^+CD8^+$/Treg ratio that was significantly increased in mice treated with anti-OX40/vaccine compared with the control ($P \leq 0.0001$) and vaccine groups ($P \leq 0.05$) were decreased significantly when anti–PD-1 was added ($P \leq 0.01$; Fig. 2H). These results collectively demonstrate that the addition of PD-1 blockade to anti-OX40/vaccine treatment negatively modulates the immune response by decreasing the number of effector $CD8^+$ T cells in the TME and abrogates the therapeutic effects obtained following OX40 costimulation with vaccine.

Anti–PD-1 enhances anti-OX40/vaccine–induced E7-specific peripheral immune responses

As shown above, combining anti–PD-1 with anti-OX40/vaccine leads to a decrease in the number of E7-specific

Downloaded from http://aacrjournals.org/cancerimmunolres/article-pdf/5/9/755/2352265/755.pdf by guest on 26 August 2022

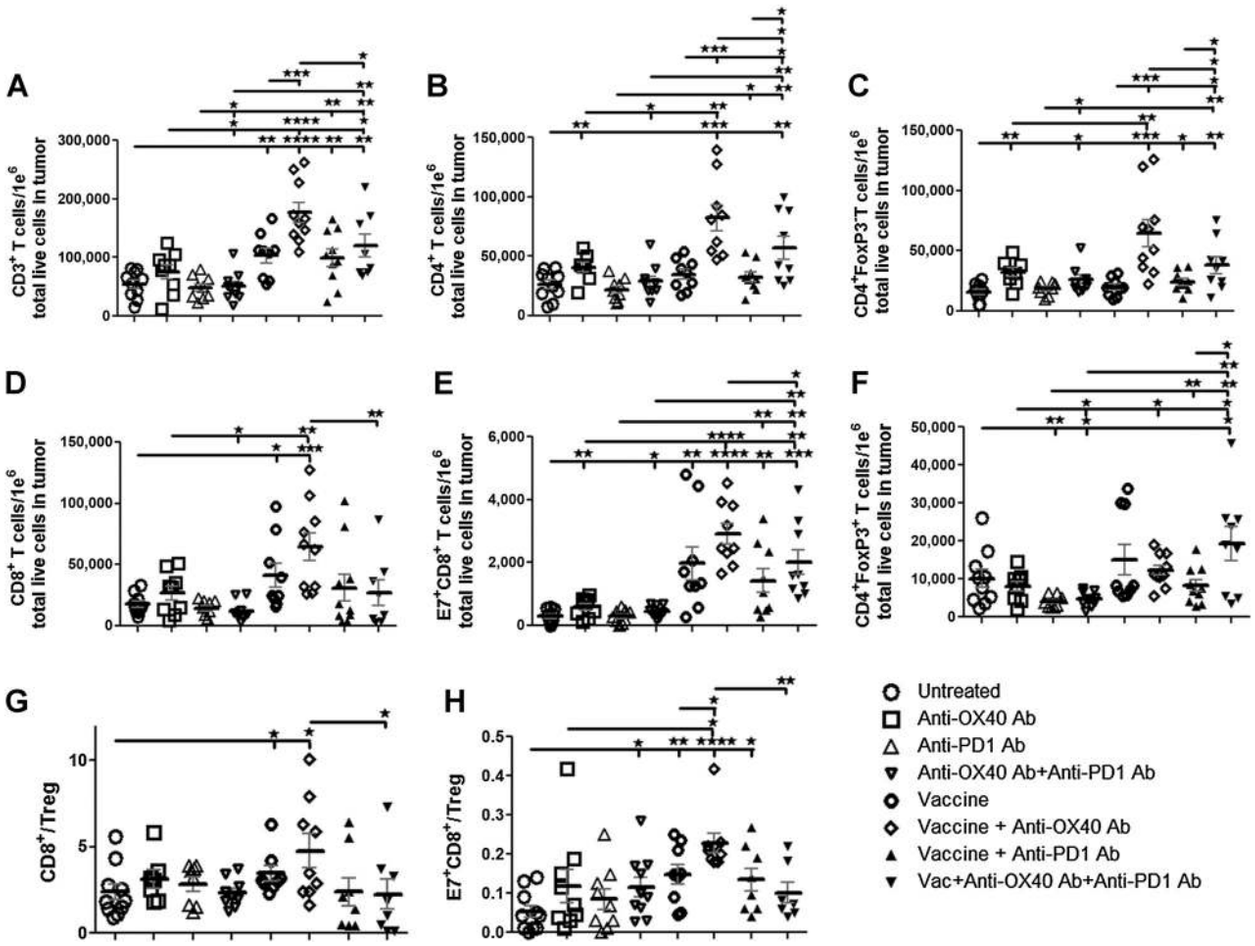

Figure 2.

Effects of the combination therapy of anti-OX40 and anti–PD-1 with tumor vaccine on tumor infiltration of effector T cells, immunosuppressive Tregs, and therapeutic ratios. C57BL/6 mice ($n = 5$ per group) were treated as in Fig. 1, except 3 days after the second vaccination, mice were sacrificed and tumors were harvested for immune response study. The absolute numbers of tumor infiltrated **A,** $CD3^+$; **B,** $CD4^+$; **C,** $CD4^+Foxp3^-$; **D,** $CD8^+$; **E,** $E7^+CD8^+$; **F,** $CD4^+Foxp3^+$ cells standardized per 1×10^6 of total live tumor cells were measured by flow cytometry. Therapeutic ratios of **G,** $CD8^+$/Tregs and **H,** $E7^+CD8^+$/Tregs are shown. Results are shown from an average of two independent experiments. *, $P \leq 0.05$; **, $P \leq 0.01$; ***, $P \leq 0.001$; ****, $P \leq 0.0001$.

$CD8^+$ T cells in the TME. To further define the immune mechanism underlying this effect, we next evaluated whether the addition of anti–PD-1 negatively affects the levels of IFNγ-producing antigen-specific $CD8^+$ T cells in spleens harvested from treated TC-1 tumor bearing mice using a standard ELISpot assay. As expected, vaccine treatment induced significant levels of IFNγ-producing E7-specific $CD8^+$ T cells compared with controls ($P \leq 0.01$; Fig. 3), which was further enhanced by addition of anti-OX40 ($P \leq 0.05$; Fig. 3). A significant increase in the numbers of IFNγ-producing E7-specific $CD8^+$ T cells was observed when anti–PD-1 was added to the anti-OX40/vaccine treatment ($P \leq 0.05$; Fig. 3). These results demonstrate that contrary to the decrease in the number of total and antigen-specific $CD8^+$ T cells in the TME, PD-1 blockade does not suppress the peripheral antigen-specific immune responses. Consequently, the peripheral effect of the combination does not explain the decrease in the number of antigen-specific $CD8^+$ T cells in the TME.

PD-1 blockade with OX40 costimulation induces apoptosis of $CD8^+$ T cells *in vitro*

Simultaneous treatment with anti–PD-1 and anti-OX40 led to a decrease in the number of total and antigen-specific $CD8^+$ T cells in the TME despite enhanced IFNγ production in the periphery by antigen-specific $CD8^+$ T cells. Therefore, we next wanted to determine the underlying mechanism of the anti–PD-1–mediated decrease in $CD8^+$ T cells.

For that purpose, we utilized the pMel-1 mouse model for *in vitro* stimulation (25). $CD8^+$ T cells from pMel-1 mice were activated with cognate gp100 peptide and the expression of PD-1, PD-L1, and OX40 was analyzed. There was a progressive increase in the expression of OX40, PD-1, and PD-L1 upon activation of cells with gp100 peptide for 48 hours compared with IL2 controls, which remained high even after resting period of 24 hours in IL2 containing medium alone (Supplementary Fig. S1A–S1C). After confirming the expression for these markers, we activated pMel-1 $CD8^+$ T cells with gp100 in the presence or

Downloaded from http://aacrjournals.org/cancerimmunolres/article-pdf/5/9/755/2352265/755.pdf by guest on 26 August 2022

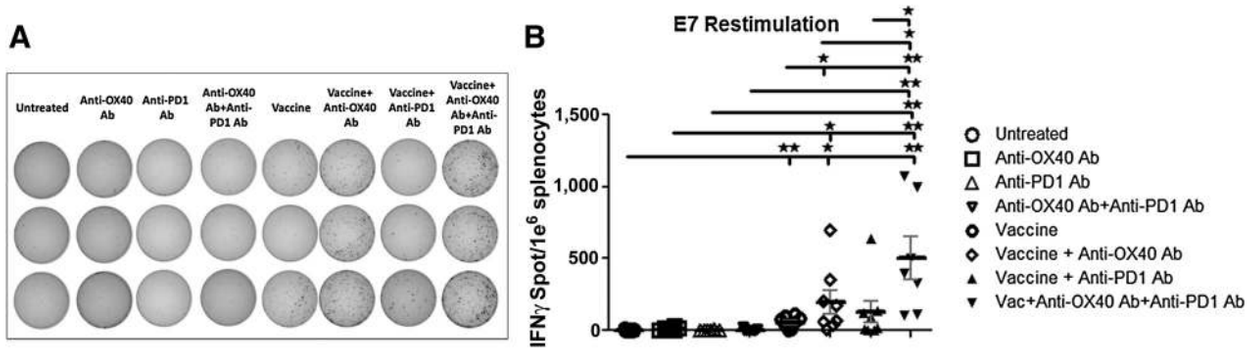

Figure 3.

Effects of the combination therapy of anti-OX40 and anti–PD-1 with tumor vaccine on tumor-specific immune response. C57BL/6 mice were treated as in Fig. 1. Antigen-specific IFNγ production was tested by ELISpot assay after restimulation of splenocytes isolated 3 days after the second vaccination from different groups with E7-specific peptide (10 μg/mL). Spots were counted using CTL Immunospot Analyzer. **A,** Representative pictures of spots obtained for three mice from each treatment group. **B,** IFNγ production was analyzed in single-cell suspensions obtained from spleens. Values representing the number of spots from E7-restimulated cultures minus that from DMSO restimulated cultures are shown. Results are shown from an average of two independent experiments. *, $P \leq 0.05$; **, $P \leq 0.01$.

absence of anti-OX40 and anti–PD-1 as outlined in Fig. 4A. We observed that under specific antigen stimulation, simultaneous addition of anti–PD-1 and anti-OX40 increased cell proliferation (Fig. 4B) compared with gp100 group (Supplementary Fig. S1D–S1F). However, this increased cell proliferation was associated with a significant increase in $CD8^+$ T-cell apoptosis ($P \leq 0.01$) as shown by increased numbers of Annexin V–positive $CD8^+$ T cells (Fig. 4C and D). Several studies have shown that OX40 enhances Bcl-xL and Bcl-2 expression and T-cell survival while suppressing apoptosis (10, 26). Therefore, we investigated the effects of different treatments on the expression of the anti-apoptotic protein, Bcl-xL. Consistent with the increase in number of Annexin V–positive apoptotic cells, we found reduced expression of pro–caspase-3 with a corresponding increase in expression of cleaved caspase-3 and decrease in Bcl-xL following addition of anti–PD-1 to the anti-OX40/vaccine (Fig. 4E). These results suggest that simultaneous blocking of PD-1/PD-L1 signaling with OX40 costimulation leads to induction of T-cell apoptosis.

We further tested *in vivo* if enhanced apoptosis is responsible for the observed decrease in the number of $CD8^+$ and antigen-specific $CD8^+$ T cells in the TME following addition of PD-1 blockade to anti-OX40/vaccine treatment. We treated mice with the same concurrent treatment schedule as outlined above for Figs. 1 and 2 and tested antigen-specific $CD8^+$ T cells for apoptosis by analyzing Annexin V–positive $E7^+CD8^+$ T cells in both spleen and tumor samples. A significant increase in the percentage of Annexin V–positive $E7^+CD8^+$ T cells out of the total number of $CD8^+$ T cells was found in the spleen of mice when treated with anti–PD-1 in combination with anti-OX40/vaccine, compared with vaccine/anti–PD-1 and anti-OX40/vaccine treatments ($P \leq 0.05$ for both; Fig. 4F). These results suggest that PD-1 blockade when combined with OX40 costimulation leads to increased proliferation and activation of antigen-specific T cells resulting in their apoptosis. A significant increase in the percentage of Annexin V–positive $E7^+CD8^+$ T cells was also observed in tumor samples obtained from mice treated with anti-OX40/vaccine combined with anti–PD-1 compared with anti–PD-1/vaccine ($P \leq 0.0001$) and anti-OX40/vaccine ($P \leq 0.001$) treatments (Fig. 4G). These results indicate that despite the enhancement of frequency of IFNγ-producing E7-specific $CD8^+$ T cells by adding anti–PD-1 to anti-OX40 in the periphery, these actively proliferating cells are rapidly undergoing apoptosis both in the periphery and in the TME.

To further explore the above findings, $CD8^+$ T cells from pMel-1 mice were treated with different sequencing of anti–PD-1 and anti-OX40 with simultaneous activation using gp100-peptide (Fig. 4H) and the effects on proliferation and apoptosis were determined. We found that only when anti–PD-1 was added to the culture concurrently with anti-OX40 (schedules 5 and 6) did proliferation ($P \leq 0.001$; Fig. 4I) and apoptosis (MFI: $P \leq 0.01$ and % Annexin V–positive: $P \leq 0.001$; Fig. 4J and K) increase significantly compared with the gp100+anti-OX40 group (schedule 2) and other groups where anti–PD-1 was not added concurrently (Supplementary Fig. S1G–S1I). This increase in proliferation and apoptosis was induced regardless of the follow-up costimulation with OX40 tested (schedules 5 and 6). This was further confirmed by demonstrating a reduction in expression of pro–caspase-3 (and increase in cleaved caspase-3) and Bcl-xL by Western analysis (schedule 2 versus 5 and 6; Fig. 4L). No significant changes in proliferation or apoptosis or expression of apoptosis-related proteins were observed when anti–PD-1 was added 24 hours after stimulation with gp100+anti-OX40 alone or in combination with continuous anti-OX40 costimulation (schedules 3 and 4) compared with gp100+anti-OX40 (schedule 2; Fig. 4H–L).

These results suggest that PD-1 blockade simultaneously with OX40 costimulation concurrent to TCR engagement with cognate antigen leads to not only increased proliferation but also significant induction of apoptosis of $CD8^+$ T cells. On the other hand, PD-1 blockade after induction of OX40 costimulation does not result in enhanced apoptosis.

PD-1 blockade post anti-OX40/vaccine treatment does not alter the antitumor effects

Our *in vitro* data suggested that, in contrast to simultaneous treatment, sequential treatment of gp100-activated $CD8^+$ T cells with anti-OX40 followed by anti–PD-1 treatment did not induce significant apoptosis or enhance proliferation of $CD8^+$ T cells

Downloaded from http://aacrjournals.org/cancerimmunolres/article-pdf/5/9/755/2352265/755.pdf by guest on 26 August 2022

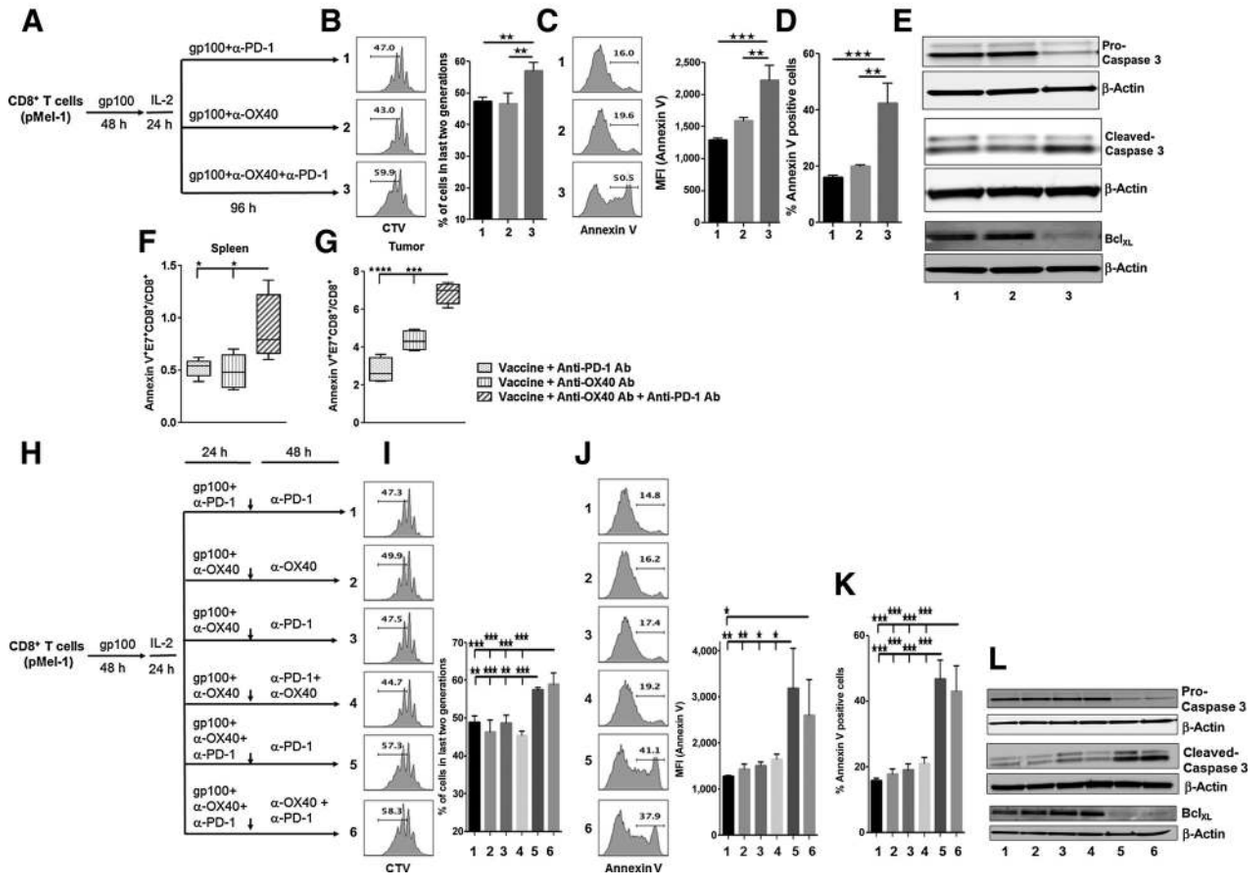

Figure 4.

Evaluation of proliferation and apoptosis in CD8$^+$ T cells *in vitro* and *in vivo*. **A,** Scheme of CD8$^+$ T-cell activation with gp100$_{25\text{-}33}$ peptide and treatment with anti–PD-1 and/or anti-OX40. Experiment was repeated twice in triplicates for each treatment schedule. **B,** Cell proliferation determined by CTV dilution. **C** and **D,** Cellular apoptosis in live-gated CD8$^+$ T-cell populations isolated from different culture conditions was analyzed by detecting Annexin V–positive cells using flow cytometry. **E,** Expression of pro–caspase-3, cleaved caspase-3, and Bcl-xL in activated CD8$^+$ T cells determined by Western blot analysis. Expression of β-actin is shown as a control. **F** and **G,** Estimation of apoptosis in live-gated CD8$^+$ T cells from spleen (**F**) or tumors (**G**) of treated mice using concurrent schedule as outlined in Fig. 1 by flow cytometry. Spleen and tumor samples were collected 3 days after second vaccination. One outlier was removed from each of the three groups in the tumor samples. The data is shown as percentage of Annexin V-positive cells in CD8$^+$ T-cell population. **H,** Scheme for sequential cell activation with gp100$_{25\text{-}33}$ peptide and treatment with anti–PD-1 and/or anti-OX40. **I,** Proliferation in activated CD8$^+$ T cells determined by CTV dilution. **J** and **K,** Apoptosis in CD8$^+$ T cells analyzed using Annexin V staining. **L,** Expression of pro–caspase-3, cleaved caspase-3, and Bcl-xL in activated CD8$^+$ T cells determined by Western blot analysis. Expression of β-actin is shown as a control. *, $P < 0.05$; **, $P < 0.01$; ***, $P < 0.001$; ****, $P < 0.0001$.

(Fig. 4). Hence, we next evaluated the effects of PD-1 blockade *in vivo* where anti–PD-1 was delayed after the administration of anti-OX40 to determine if different sequencing of treatments could enhance the antitumor efficacy. Mice were implanted with TC-1 cells on day 0 and agonist OX40 Ab was administered with the peptide vaccine starting on day 12 and either continued throughout the experiment (αOX40-C; Fig. 5A) or given for short-term until day 19 and then discontinued (αOX40-ST; Fig. 5E). Anti–PD-1 was administered at the time of the second vaccination (day 19; αPD1-L; Fig. 5A and E). Similar to the *in vitro* results, PD-1 blockade following anti-OX40 and vaccine treatment was not detrimental to anti-OX40 treatment, but did not show any additive or negative effects on tumor growth and survival compared with the anti-OX40/vaccine treatment with (Fig. 5B–D) or without (Fig. 5F–H) continuation of OX40 costimulation.

These results are consistent with the *in vitro* stimulation experiments outlined above and demonstrate that adding anti–PD-1 after administration of anti-OX40/vaccine treatment does not result in inhibition of the effect of anti-OX40/vaccine treatment.

Anti-OX40/vaccine effects on T-cell clonality and tumor infiltration are negated by anti–PD-1

To further examine the effects of adding anti–PD-1 to anti-OX40/vaccine treatment, we performed high-throughput immunoSequencing on the β chain locus of T cells from tumor and spleen samples in mice treated with each therapy alone or in combination. We sequenced an average of 157,836 (range: 28,160–457,940) and 48,821 (range: 3,530–307,535) TCRs in spleen and tumor, respectively, providing a quantitative snapshot of the relative abundance of each T-cell in a sample. The shape of this T-cell frequency distribution, summarized by the clonality

Downloaded from http://aacrjournals.org/cancerimmunolres/article-pdf/5/9/755/2352265/755.pdf by guest on 26 August 2022

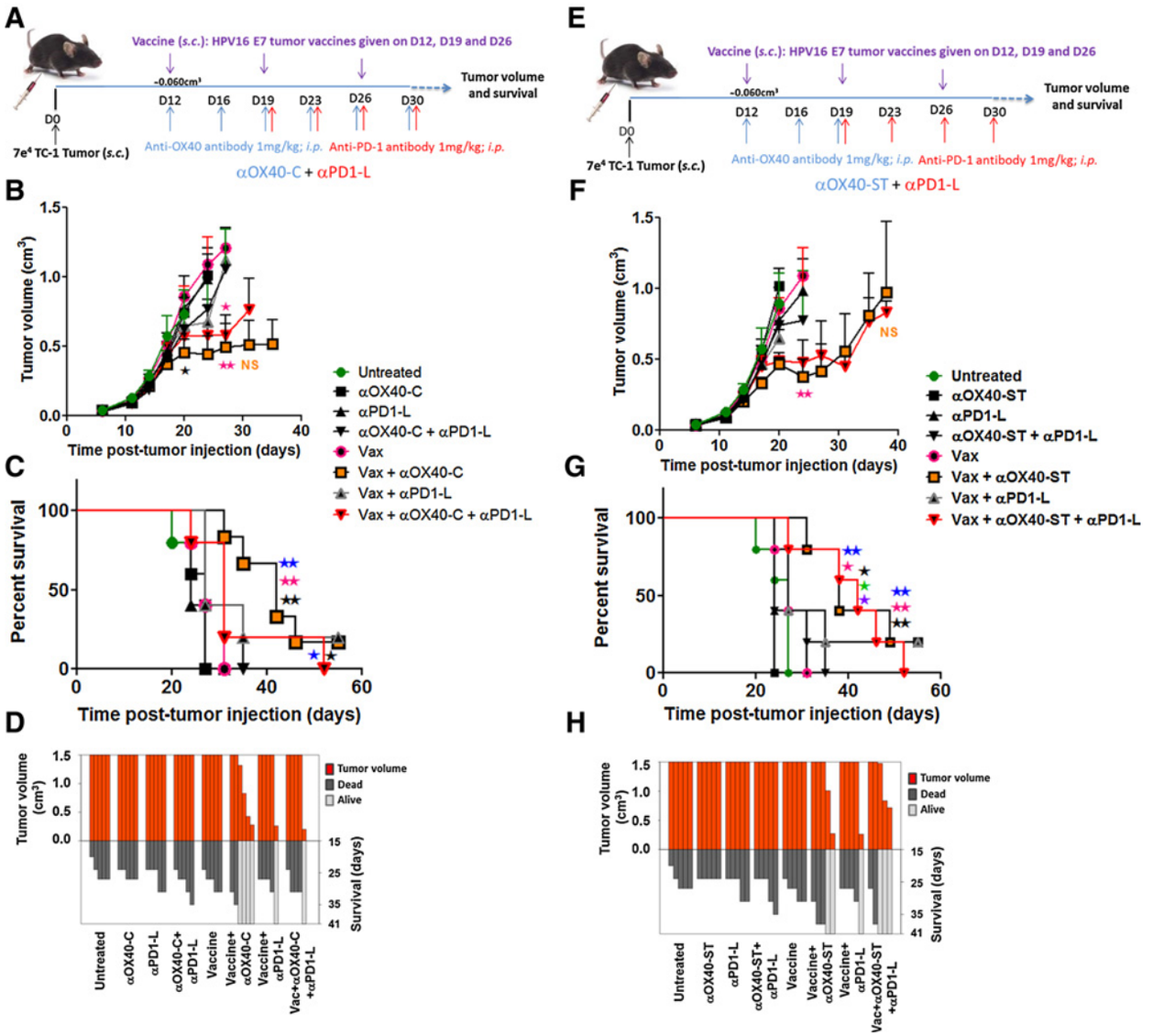

Figure 5.

Effects of delayed scheduling of anti–PD-1 on tumor growth and survival. **A,** Schematic representation of the treatment schedule in TC-1 mouse tumor model. On day 12 of tumor growth, TC-1 tumor-bearing mice were given anti-OX40 (1 mg/kg, i.p., twice weekly) throughout the experiment (αOX40-C) along with HPV17 $E7_{49\text{-}57}$ peptide vaccine (s.c., every 7 days for a total of 3 doses). Administration of anti–PD-1 was delayed (αPD-1-L) beginning from day 19. Tumor growth and survival were measured. **B,** Averaged tumor volumes following various treatments ($n = 5$ per group). **C,** Percent survival of mice depicted by the Kaplan–Meier plot. **D,** SK plot showing the tumor volume and survival for each mouse at different days. **E,** Schematic representation of the treatment schedule where tumor-bearing mice were treated similarly as described in **A** except anti-OX40 was administered only until D19 (αOX40-ST). **F,** Averaged tumor volumes following various treatments ($n = 5$ per group). **G,** Percent survival of mice depicted by Kaplan–Meier plot. **H,** SK plot showing the tumor volume and survival for each mouse at different days. Similar results were obtained from two independent experiments. *, $P \leq 0.05$; **, $P \leq 0.01$; ***, $P \leq 0.001$; ****, $P \leq 0.0001$; *vs. UT, *vs. vaccine, *vs. anti-OX40, *vs. anti–PD-1, *vs. anti-OX40 + anti–PD-1, *vs. vaccine + anti-OX40; i.p., intraperitoneal; s.c., subcutaneous.

metric, correlated with treatment outcome in an immunotherapy setting (27), where a highly skewed repertoire and higher clonality indicate mono- or oligo-clonal expansion of T cells responding to therapy. In both spleen and tumor, we observed significantly greater clonality in the anti-OX40/vaccine group compared with mice in the untreated control ($P \leq 0.01$), anti-OX40 ($P \leq 0.05$), and anti–PD-1 ($P \leq 0.01$) groups (Fig. 6A). T-cell infiltration was also significantly greater following anti-OX40/vaccine treatment in tumors but not in spleen compared with untreated control, anti-OX40, anti–PD-1 ($P \leq 0.0001$ for each), and the vaccine group ($P \leq 0.001$; Fig. 6B). Further, we observed a significant decrease in clonality ($P \leq 0.05$ for tumor and spleen) and T-cell fraction ($P \leq 0.001$ in tumor) following addition of PD-1 blockade to anti-OX40/vaccine treatment compared with the anti-OX40/vaccine group (Fig. 6A and B). Clonality and T-cell fraction were also correlated across tumors (Supplementary Fig. S2A)

Downloaded from http://aacrjournals.org/cancerimmunolres/article-pdf/5/9/755/2352265/755.pdf by guest on 26 August 2022

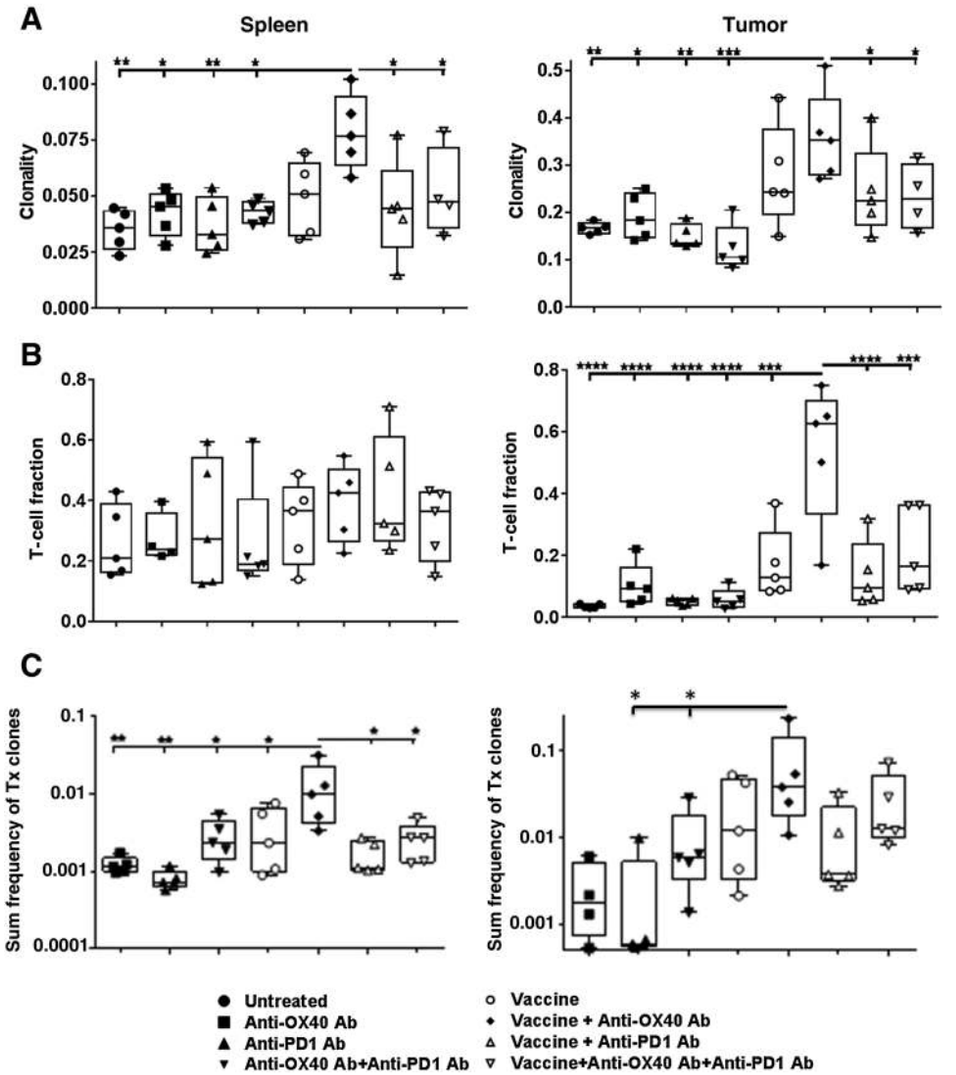

Figure 6.
Effects of the combination therapy of anti-OX40 and anti–PD-1 with tumor vaccine on spleen and tumor T-cell infiltration and clonality. ImmunoSequencing of the TCRβ locus was performed on spleen and tumor tissues collected 3 days after second vaccination (from 5 mice/group). An average of 157,836 and 48,821 T-cell receptors in spleen and tumor, respectively, were sequenced and **A,** T-cell clonality, and **B,** T-cell infiltration were characterized. **C,** The frequency of vaccine + anti-OX40 treatment-associated clones identified in the tumor.

suggesting that the antitumor response in these mice consisted mainly of the expansion of a small number of specific T cells. In order to assess the possibility of common TCRs being generated against the tumor in anti-OX40Ab/vaccine-treated mice, we compared CDR3 amino acid sequences across different mice. We defined 41 public T cells that may be responding to treatment as CDR3 amino acid sequences that were present in the top 500 most frequent tumor T-cell clones of at least two mice treated with anti-OX40/vaccine, but not present in any of the untreated mice (Fig. 6C). We found that these T cells were present at lower frequencies in the tumors of mice treated with anti–PD-1 or anti-OX40+anti-PD-1 ($P \leq 0.05$). In spleen, these patterns held true for the anti–PD-1 and anti-OX40 groups, although we also saw a significant decrease in clone frequencies in the mice treated with anti–PD-1/vaccine or vaccine+anti-OX40+anti–PD-1 groups ($P \leq 0.05$; Fig. 6C). For comparison, we also identified clones using the same criteria for the vaccine+anti-OX40+anti–PD-1 treatment group and another set of clones present in the top 500 of at least two untreated mice (Supplementary Fig. S2B and S2C). Both of these groups show different patterns of frequency across mice. For instance, the anti–PD-1/vaccine group had higher frequencies of the clones associated with the vaccine+anti-OX40+anti–PD-1 treatment group than the anti-OX40/vaccine group. These data indicate that the T-cell response induced by the anti-OX40/vaccine treatment is distinct from that induced in the untreated controls or the vaccine+anti-OX40+anti–PD-1 treatment group. Together, these data obtained through immunoSequencing are consistent with immune cell infiltration in the TME (Fig. 2), demonstrating that concurrent addition of PD-1 blockade attenuates the antitumor effects of anti-OX40/vaccine treatment and that these effects may be mediated through apoptosis of antigen-specific T cells.

Discussion

The use of checkpoint-inhibitor Abs against PD-1/PD-L1 has led to improvement in the survival of cancer patients, although only in <40% of the cases and in a few types of cancers (3–5). The generation of a strong immune response is essential to enhance the effects of immunotherapy. Several agonist costimulatory Abs have been utilized both in preclinical and clinical studies for this purpose (7–10). Accordingly, development of

Downloaded from http://aacrjournals.org/cancerimmunolres/article-pdf/5/9/755/2352265/755.pdf by guest on 26 August 2022

combination strategies utilizing different immune modulators, including agonist costimulatory Abs and checkpoint inhibitor Abs, is needed (3–6). Because anti-OX40 agonist Ab, already in early phase clinical trials (8), generates strong immune responses (8–10), the combination of anti–PD-1/PD-L1 Ab and anti-OX40 is an obvious choice for combination immunotherapy. A few clinical trials have already started; others are in the planning stage to test this combination (12, 13). However, the immune effect of such a combination and the interaction of the two molecules on the downstream immune outcome remain unclear.

Here, we discovered that addition of anti–PD-1 exhibits a detrimental effect on the anti-OX40 agonist Ab-mediated tumor response when combined in a therapeutic approach. As expected, anti-OX40 significantly increased E7-specific $CD8^+$ T cells induced by the HPV E7 vaccine, leading to an antitumor response and prolonged survival of tumor bearing mice. We hypothesized that combining the PD-1 blockade with anti-OX40 treatment could improve the antitumor immune response, leading to a better therapeutic outcome. However, we found that, despite the fact that the addition of PD-1 blockade concurrently with anti-OX40 enhanced the antigen-specific peripheral immune response, it negated the antitumor effects mediated by OX40 costimulation. Addition of anti–PD-1 abrogated the increase in the numbers of infiltrated $CD4^+$, $CD8^+$, and E7-specific $CD8^+$ T cells in the TME induced by anti-OX40/vaccine and resulted in decreased therapeutic ratios of $CD8^+$/Tregs and $E7^+CD8^+$/Tregs. As addition of the PD-1 blockade to anti-OX40/vaccine treatment resulted in reduction of $CD8^+$ and antigen-specific $CD8^+$ T cells in the TME, we asked whether numbers of IFNγ-producing antigen-specific $CD8^+$ T cells were reduced following concurrent treatment of anti-OX40 and anti–PD-1. We found that the combination of anti-OX40 and anti–PD-1 actually enhanced antigen-specific T-cell activation and IFNγ production in the periphery compared with anti-OX40.

In a plasmodium-infected rodent model, OX40-mediated signaling enhanced helper $CD4^+$ T-cell activity, humoral immunity and parasite clearance (28). This effect was abrogated following simultaneous PD-1 blockade because the combination resulted in excessive induction of IFNγ secretion that impaired T helper cell-mediated humoral immunity and parasite control (28). Overexpression of IFNγ leads to activation-induced cell death of lymphocytes (29–31). Further, PD-1 blockade can reverse T-cell suppression and exhaustion (32, 33). As we found that the concomitant treatment with anti-OX40 and anti–PD-1 enhances IFNγ production, we hypothesized that the combination of these Abs will lead to apoptosis of $CD8^+$ T cells. Indeed, our results demonstrate that blocking PD-1/PD-L1 signaling concomitantly with initiation of antigen stimulation and OX40 costimulation leads to an increase in apoptosis of antigen-specific $CD8^+$ T cells *in vitro*. We also observed a reduction in the expression of pro–caspase-3 and anti-apoptotic Bcl-xL proteins in treated cells. Concomitant treatment with anti–PD-1 at the time of initiation of anti-OX40 treatment with vaccine resulted in apoptosis of $E7^+CD8^+$ T cells in both tumors and spleens *in vivo*. These findings indicate that PD-1 signaling is required during early T-cell activation and proliferation mediated by anti-OX40. These data also suggest that simultaneous OX40 costimulation and PD-1 pathway blockade lead to increased activation and proliferation of T cells, resulting in their apoptosis both in the periphery and in the TME.

ImmunoSequencing and analysis of the tumor and spleen T-cell repertoires returned analyses consistent with increased apoptosis after addition of PD-1 blockade. Analyses of T-cell infiltration revealed a significant reduction in the T-cell fraction in the TME following addition of PD-1 blockade to anti-OX40/vaccine treatment. The clonality of the T-cell repertoire in a TME quantitates the expansion of clones that may be responding to antigens. Increases in clonality in the TME post- anti–PD-1/anti-CTLA-4 therapy have correlated with response (34) and clonality in the pretreatment TME is a predictive biomarker of response to anti–PD-1 treatment (27). Here, we observed a trend toward decreased clonality when PD-1 blockade was added to anti-OX40/vaccine treatment, suggesting that antigen-specific T cells are at lower frequencies in these mice. Upon identifying a set of T cells that may be antigen-specific in the mice treated with anti-OX40/vaccine, we found that these T-cell clones trended toward a lower frequency after the addition of PD-1 blockade. In the future, sequencing of antigen (E7)-specific T cells may provide corroborating evidence for this hypothesis.

Our results demonstrate that addition of PD-1 blockade is detrimental for therapeutic outcomes when combined with anti-OX40 and vaccine at the initiation of therapy. However, addition of anti–PD-1 in a delayed schedule, whether sequential or overlapping, did not exhibit the same negative effect on anti-OX40. Our *in vitro* data were consistent with our *in vivo* findings. *In vitro* pMel-1 $CD8^+$ T-cell stimulation experiments show that contrary to when anti–PD-1 and anti-OX40 were added simultaneously, addition of anti–PD-1 after the initial costimulation with anti-OX40 and antigen does not lead to apoptosis of $CD8^+$ T cells. Similarly, we found that the delayed administration of anti–PD-1 did not result in a therapeutic benefit.

Several mechanisms may underlie the effect of treatment schedules on therapeutic outcome. For example, PD-1–induced TCR-mediated signaling alters dynamics of contact interactions between T cells and antigen-bearing dendritic cells (DCs; ref. 35). It is possible that a different sequencing of PD-1 blockade or addition of PD-1 blockade to other therapies modulate the interaction of T cells with the DCs so the T cells remain migratory and become anergic. PD-1 signaling is also involved in altering T-cell metabolism. Activated T cells receiving signals from PD-1 have a more oxidative environment, leading to PD-1–mediated T-cell dysfunction during chronic infections and cancer (35). PD-L1 expression is also associated with cancer cell-intrinsic signaling through the PI3K/Akt/mTOR pathway, leading to enhanced glycolytic metabolism in cancer cells (35). The scheduling of PD-1 blockade before, during, and after vaccine or anti-OX40 may alter these signaling events leading to modulation of metabolism and the effector function of T cells.

Our results may not be applicable to other checkpoint inhibitor combinations with anti-OX40. A combination of anti-OX40 and anti-CTLA-4 Abs with peptide vaccine induces expansion of tumor-specific pMel-1 $CD8^+$ T cells (36). And, in a spontaneous tumor model where a combination of anti-OX40 and anti-CTLA-4 Abs induced T-cell anergy, addition of vaccine overcomes T-cell anergy, promotes expansion of effector T cells, and augments Th1 cytokine-producing $CD8^+$ T cells (36). However, that study did not report the effects of combination of vaccine and anti-OX40 on tumor growth, survival or immune response making the comparison with our results problematic.

We show that simultaneous blockade of PD-1 and costimulation of OX40 has an adverse effect on the antitumor activity of

Downloaded from http://aacrjournals.org/cancerimmunolres/article-pdf/5/9/755/2352265/755.pdf by guest on 26 August 2022

OX40 costimulation. Our data has important implications for cancer immunotherapy, particularly the combination of anti–PD-1 and anti-OX40. Based on these results, the identification of optimum sequencing for targeting immune checkpoint modulators in combination immunotherapy of cancer is critical to achieve a maximum, long-lasting response, and clinical success.

Disclosure of Potential Conflicts of Interest

R.M. Gittelman is a computational biologist at Adaptive Biotechnologies. E. Yusko is a computational biologist, manager, at Adaptive Biotechnologies. C. Sanders has ownership interest in Adaptive Biotechnologies. H. Robins is cofounder of Adaptive Biotechnologies and has ownership interest in the same. S.A. Hammond has ownership interest in AstraZeneca/MedImmune. M. Mkrtichyan is a scientist at FivePrime Therapeutics Inc. S.N. Khleif reports receiving a commercial research grant from MedImmune. No potential conflicts of interest were disclosed by the other authors.

Authors' Contributions

Conception and design: R.K. Shrimali, S. Ahmad, C. Sanders, S.A. Hammond, S.N. Khleif

Development of methodology: R.K. Shrimali, S. Ahmad, V. Verma, H. Robins, J.E. Janik, M. Mkrtichyan, S.N. Khleif

Acquisition of data (provided animals, acquired and managed patients, provided facilities, etc.): R.K. Shrimali, S. Ahmad, V. Verma, S. Ananth, P. Gaur, S.N. Khleif

Analysis and interpretation of data (e.g., statistical analysis, biostatistics, computational analysis): R.K. Shrimali, S. Ahmad, V. Verma, R.M. Gittelman, E. Yusko, C. Sanders, S.A. Hammond, J.E. Janik, M. Mkrtichyan, S. Gupta, S.N. Khleif

Writing, review, and/or revision of the manuscript: R.K. Shrimali, S. Ahmad, V. Verma, R.M. Gittelman, E. Yusko, S.A. Hammond, J.E. Janik, M. Mkrtichyan, S. Gupta, S.N. Khleif

Administrative, technical, or material support (i.e., reporting or organizing data, constructing databases): R.K. Shrimali, P. Zeng, S. Gupta, S.N. Khleif

Study supervision: R.K. Shrimali, S.N. Khleif

Acknowledgments

The authors thank Dr. Rhea-Beth Markowitz for editing the manuscript.

The costs of publication of this article were defrayed in part by the payment of page charges. This article must therefore be hereby marked *advertisement* in accordance with 18 U.S.C. Section 1734 solely to indicate this fact.

Received June 8, 2017; revised June 21, 2017; accepted July 18, 2017; published OnlineFirst August 28, 2017.

References

1. Chen L, Flies DB. Molecular mechanisms of T cell co-stimulation and co-inhibition. Nat Rev Immunol 2013;13:227–42.
2. Zhu Y, Yao S, Chen L. Cell surface signaling molecules in the control of immune responses: a tide model. Immunity 2011;34:466–78.
3. Page DB, Postow MA, Callahan MK, Allison JP, Wolchok JD. Immune modulation in cancer with antibodies. Annu Rev Med 2014;65:185–202.
4. Zou W, Wolchok JD, Chen L. PD-L1 (B7-H1) and PD-1 pathway blockade for cancer therapy: mechanisms, response biomarkers, and combinations. Sci Transl Med 2016;8:328rv4.
5. Hamanishi J, Mandai M, Matsumura N, Abiko K, Baba T, Konishi I. PD-1/PD-L1 blockade in cancer treatment: perspectives and issues. Int J Clin Oncol 2016;21:462–73.
6. Wolchok JD, Kluger H, Callahan MK, Postow MA, Rizvi NA, Lesokhin AM, et al. Nivolumab plus ipilimumab in advanced melanoma. N Engl J Med 2013;369:122–33.
7. Sanmamed MF, Pastor F, Rodriguez A, Perez-Gracia JL, Rodriguez-Ruiz ME, Jure-Kunkel M, et al. Agonists of Co-stimulation in cancer immunotherapy directed against CD137, OX40, GITR, CD27, CD28, and ICOS. Semin Oncol 2015;42:640–55.
8. Aspeslagh S, Postel-Vinay S, Rusakiewicz S, Soria JC, Zitvogel L, Marabelle A. Rationale for anti-OX40 cancer immunotherapy. Eur J Cancer 2016;52:50–66.
9. Linch SN, McNamara MJ, Redmond WL. OX40 agonists and combination immunotherapy: putting the pedal to the metal. Front Oncol 2015;5:34.
10. Croft M, So T, Duan W, Soroosh P. The significance of OX40 and OX40L to T-cell biology and immune disease. Immunol Rev 2009;229:173–91.
11. Bansal-Pakala P, Halteman BS, Cheng MH, Croft M. Costimulation of CD8 T cell responses by OX40. J Immunol 2004;172:4821–5.
12. Infante JR HA, Pishvaian MJ, Chow LQM, McArthur GA, Bauer TM, Liu SV, et al. A phase Ib dose escalation study of the OX40 agonist MOXR0916 and the PD-L1 inhibitor atezolizumab in patients with advanced solid tumors. J Clin Oncol 2016;34:suppl; abstr 101.
13. April 15, 2017. ClinicalTrials.gov. <https://clinicaltrials.gov/ct2/results?term=ox40&Search=Search>. Accessed 2017 April 15, 2017.
14. Abu Eid R, Friedman KM, Mkrtichyan M, Walens A, King W, Janik J, et al. Akt1 and -2 inhibition diminishes terminal differentiation and enhances central memory CD8+ T-cell proliferation and survival. Oncoimmunology 2015;4:e1005448.
15. Lin KY, Guarnieri FG, Staveley-O'Carroll KF, Levitsky HI, August JT, Pardoll DM, et al. Treatment of established tumors with a novel vaccine that enhances major histocompatibility class II presentation of tumor antigen. Cancer Res 1996;56:21–6.
16. Ahmad S, Abu-Eid R, Shrimali R, Webb M, Verma V, Doroodchi A, et al. Differential PI3Kdelta signaling in CD4+ T-cell subsets enables selective targeting of T regulatory cells to enhance cancer immunotherapy. Cancer Res 2017;77:1892–904.
17. Robins HS, Campregher PV, Srivastava SK, Wacher A, Turtle CJ, Kahsai O, et al. Comprehensive assessment of T-cell receptor beta-chain diversity in alphabeta T cells. Blood 2009;114:4099–107.
18. Robins H, Desmarais C, Matthis J, Livingston R, Andriesen J, Reijonen H, et al. Ultra-sensitive detection of rare T cell clones. J Immunol Methods 2012;375:14–9.
19. Carlson CS, Emerson RO, Sherwood AM, Desmarais C, Chung MW, Parsons JM, et al. Using synthetic templates to design an unbiased multiplex PCR assay. Nat Commun 2013;4:2680.
20. Kirsch I, Vignali M, Robins H. T-cell receptor profiling in cancer. Mol Oncol 2015;9:2063–70.
21. Curran MA, Montalvo W, Yagita H, Allison JP. PD-1 and CTLA-4 combination blockade expands infiltrating T cells and reduces regulatory T and myeloid cells within B16 melanoma tumors. Proc Natl Acad Sci USA 2010;107:4275–80.
22. Shen Z, Zhou S, Wang Y, Li RL, Zhong C, Liang C, et al. Higher intratumoral infiltrated Foxp3+ Treg numbers and Foxp3+/CD8+ ratio are associated with adverse prognosis in resectable gastric cancer. J Cancer Res Clin Oncol 2010;136:1585–95.
23. Biller BJ, Guth A, Burton JH, Dow SW. Decreased ratio of CD8+ T cells to regulatory T cells associated with decreased survival in dogs with osteosarcoma. J Vet Intern Med 2010;24:1118–23.
24. Watanabe Y, Katou F, Ohtani H, Nakayama T, Yoshie O, Hashimoto K. Tumor-infiltrating lymphocytes, particularly the balance between CD8(+) T cells and CCR4(+) regulatory T cells, affect the survival of patients with oral squamous cell carcinoma. Oral Surg Oral Med Oral Pathol Oral Radiol Endod 2010;109:744–52.
25. Overwijk WW, Tsung A, Irvine KR, Parkhurst MR, Goletz TJ, Tsung K, et al. gp100/pmel 17 is a murine tumor rejection antigen: induction of "self"-reactive, tumoricidal T cells using high-affinity, altered peptide ligand. J Exp Med 1998;188:277–86.
26. Rogers PR, Song J, Gramaglia I, Killeen N, Croft M. OX40 promotes Bcl-xL and Bcl-2 expression and is essential for long-term survival of CD4 T cells. Immunity 2001;15:445–55.

Downloaded from http://aacrjournals.org/cancerimmunolres/article-pdf/5/9/755/2352265/755.pdf by guest on 26 August 2022

27. Tumeh PC, Harview CL, Yearley JH, Shintaku IP, Taylor EJ, Robert L, et al. PD-1 blockade induces responses by inhibiting adaptive immune resistance. Nature 2014;515:568–71.
28. Zander RA, Obeng-Adjei N, Guthmiller JJ, Kulu DI, Li J, Ongoiba A, et al. PD-1 Co-inhibitory and OX40 Co-stimulatory crosstalk regulates helper T cell differentiation and anti-plasmodium humoral immunity. Cell Host Microbe 2015;17:628–41.
29. Refaeli Y, Van Parijs L, Alexander SI, Abbas AK. Interferon gamma is required for activation-induced death of T lymphocytes. J Exp Med 2002;196:999–1005.
30. Lohman BL, Welsh RM. Apoptotic regulation of T cells and absence of immune deficiency in virus-infected gamma interferon receptor knockout mice. J Virol 1998;72:7815–21.
31. Dondi E, Roue G, Yuste VJ, Susin SA, Pellegrini S. A dual role of IFN-alpha in the balance between proliferation and death of human CD4+ T lymphocytes during primary response. J Immunol 2004;173:3740–7.
32. Trautmann L, Janbazian L, Chomont N, Said EA, Gimmig S, Bessette B, et al. Upregulation of PD-1 expression on HIV-specific CD8+ T cells leads to reversible immune dysfunction. Nat Med 2006;12:1198–202.
33. Day CL, Kaufmann DE, Kiepiela P, Brown JA, Moodley ES, Reddy S, et al. PD-1 expression on HIV-specific T cells is associated with T-cell exhaustion and disease progression. Nature 2006;443:350–4.
34. Weber J, Horak C, Hodi FS, Chang H, Woods D, Sanders C, et al. Baseline tumor T cell receptor (TcR) sequencing analysis and neo antigen load is associated with benefit in melanoma patients receiving sequential nivolumab and ipilimumab. Ann Oncol 2016;27.
35. Boussiotis VA. Molecular and biochemical aspects of the PD-1 checkpoint pathway. N Engl J Med 2016;375:1767–78.
36. Linch SN, Kasiewicz MJ, McNamara MJ, Hilgart-Martiszus IF, Farhad M, Redmond WL. Combination OX40 agonism/CTLA-4 blockade with HER2 vaccination reverses T-cell anergy and promotes survival in tumor-bearing mice. Proc Natl Acad Sci USA 2016;113:E319–27.

Downloaded from http://aacrjournals.org/cancerimmunolres/article-pdf/5/9/755/2352265/755.pdf by guest on 26 August 2022